

Supplementary Information to

## Measurement of Quantum Coherence in Thin Films of Molecular Quantum Bits without Post-Processing

Samuel Lenz, Bastian Kern, Martin Schneider and Joris van Slageren

**Pulsed Q-Band Measurements.** Echo detected EPR spectra were recorded by recording the Hahn echo intensity following the  $(\pi/2-\tau-\pi-\tau-\text{echo})$ -pulse sequence as a function of field. The same sequence was used to determine the phase memory time by varying the interpulse delay time  $\tau$ . The spin-lattice relaxation time of the CuPc sample was determined by the  $(\pi-\tau-\pi/2-\tau-\pi-\tau-\text{echo})$ -inversion recovery sequence. In the case of the BDPA samples, it proved impossible to invert the magnetization due to the size of the sample. Instead, the spin-lattice relaxation time was determined by varying the repetition time of the Hahn echo sequence, allowing extraction of  $T_1$  by the saturation behaviour of the echo intensity. Nutation measurements were performed by varying  $\tau_{\text{nut}}$  in the nutation  $(\tau_{\text{nut}}-\pi/2-\tau-\pi-\tau-\text{echo})$ -sequence.

**FPR Construction.** The resonator was made from brass and features a concave top mirror with a radius of curvature of 43 mm and a coupling hole (2.5 mm diameter). The bottom mirror is flat, both mirrors have a diameter of 37 mm. The waveguide is sealed with a sheet of mica and made out of steel in order to reduce heat conduction.

**Microwave Simulations.** Microwave Simulations were carried out using CST Studio 2018. The Fabry-Pérot resonator was modelled as built and the Eigenmode Solver of CST Studio was used to simulate the field distributions of the different modes. A tetrahedral mesh in combination with the mesh refinement (frequency deviation of the modes  $> 0.001$  GHz) was used.



**Figure S 1:** Opened, manufactured FPR with a 5 mm diameter sample mounted.



**Figure S 2:** Closed FPR, the flange on the top complies with our flow cryostat

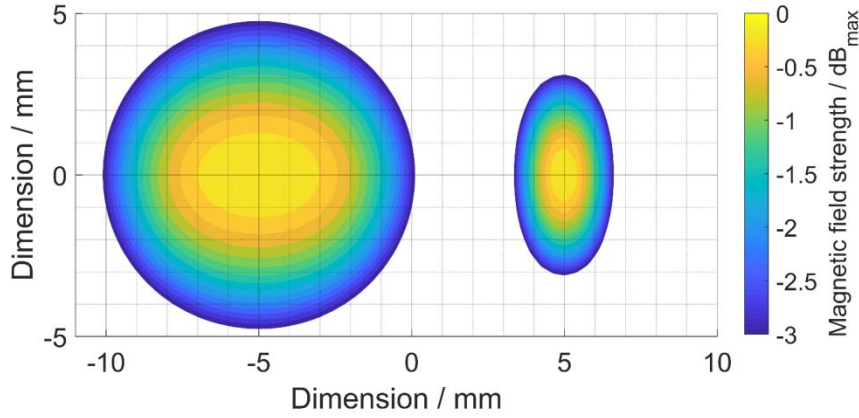


**Figure S 3:** 2D magnetic field distribution at the bottom mirror of the fourth mode occurring at 35 GHz in our FPR (left) simulated with CST Studio. On the right, a 2D magnetic field distribution of the typical TE<sub>011</sub> mode at 35 GHz occurring in a CR is shown. The area of the FPR mode is five times larger compared to the CR mode.

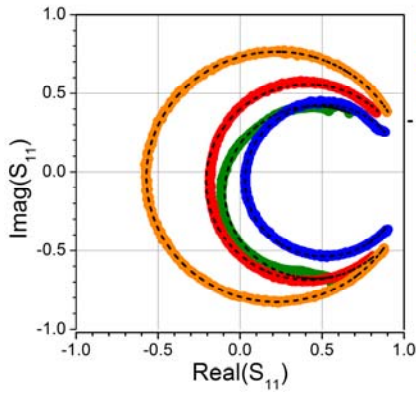


**Figure S 4** Measured  $Q$ -circles of the different modes occurring in the FPR (coloured symbols) fitted with a circle (black dotted line)

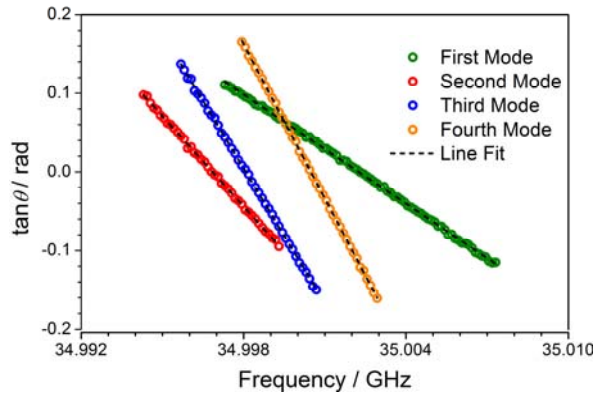


**Figure S 5:** Linearized measured reflection data (coloured symbols, see text and ref 16 for details) fitted with a straight line (black dotted line).

**Table S 1: Intermirror distance, measured  $Q$ -factors and coupling coefficient of the different modes occurring in the FPR**

Mode	Intermirror distance / mm	$Q_{\text{unloaded}}$	$Q_{\text{external}}$	$Q_{\text{loaded}}$	$K$
First mode (TEM <sub>001</sub> + TM <sub>311</sub> )	4.7	$900 \pm 40$	$723 \pm 10$	$404 \pm 1$	$1.2 \pm 0.1$
Second mode (TEM <sub>101</sub> + TM <sub>111</sub> )	5.8	$1700 \pm 60$	$1050 \pm 50$	$648 \pm 3$	$1.70 \pm 0.04$
Third mode (TEM <sub>201</sub> + TM <sub>211</sub> )	7.2	$1930 \pm 30$	$2060 \pm 20$	$997 \pm 3$	$0.93 \pm 0.02$
Fourth mode (TEM <sub>002</sub> )	9.2	$5560 \pm 20$	$1437 \pm 15$	$1142 \pm 2$	$3.87 \pm 0.01$

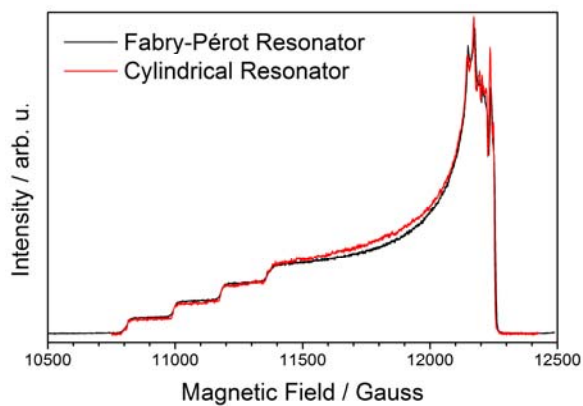


**Figure S 6** Echo detected EPR-spectrum of 0.1% Cu(dbm)<sub>2</sub> in Pd(dbm)<sub>2</sub> at 35 GHz and 7K in recorded with our FPR (black line) and CR (red line)

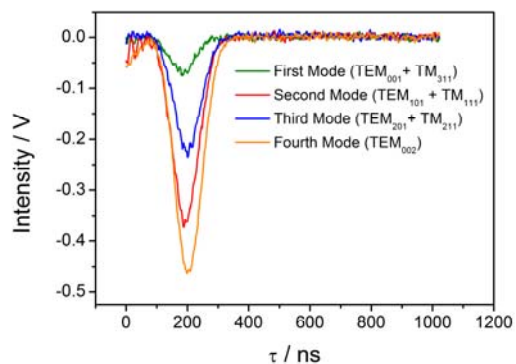


**Figure S 7** Hahn-Echos of 5% BDPA in Polystyrene (5mm diameter, 0.1mm thick) at 35 GHz, 293 K and 12489 G using different modes in our FPR.

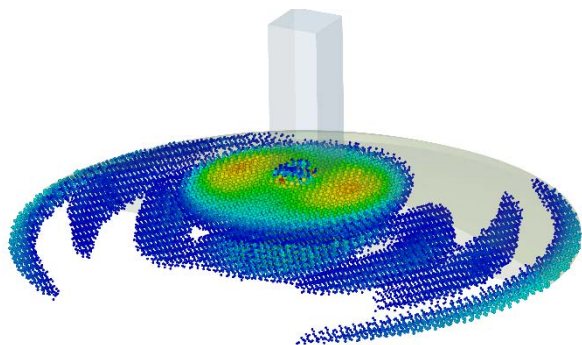


**Figure S 8:** 3D magnetic field distribution of the first mode occurring at 35 GHz in our FPR.

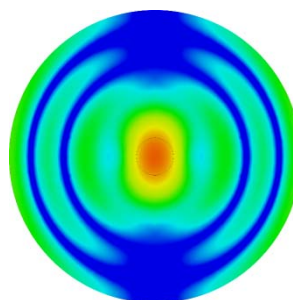


**Figure S 9:** Simulated 2D magnetic field distribution at the bottom mirror of the first mode occurring at 35 GHz in our FPR.

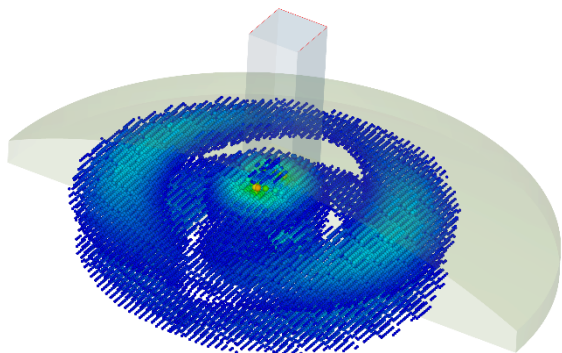


**Figure S 10:** 3D magnetic field distribution of the second mode occurring at 35 GHz in our FPR.

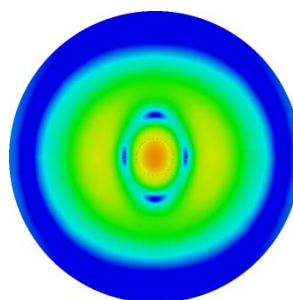


**Figure S 11:** 2D magnetic field distribution at the bottom mirror of the second mode occurring at 35 GHz in our FPR simulated .

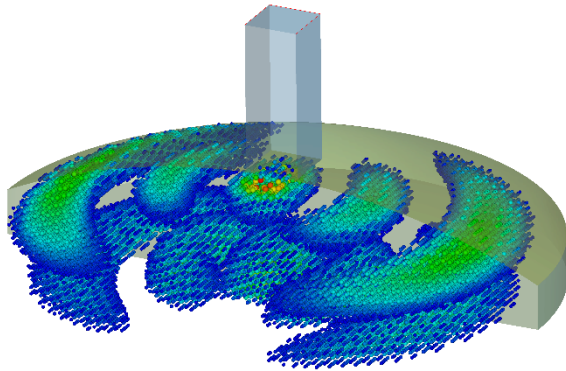


**Figure S 12:** 3D magnetic field distribution of the third mode occurring at 35 GHz in our FPR.

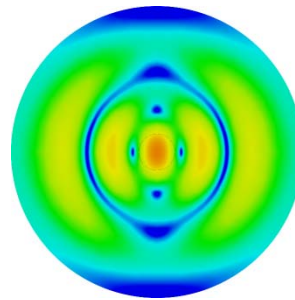


**Figure S 13:** 2D magnetic field distribution at the bottom mirror of the third mode occurring at 35 GHz in our FPR simulated .

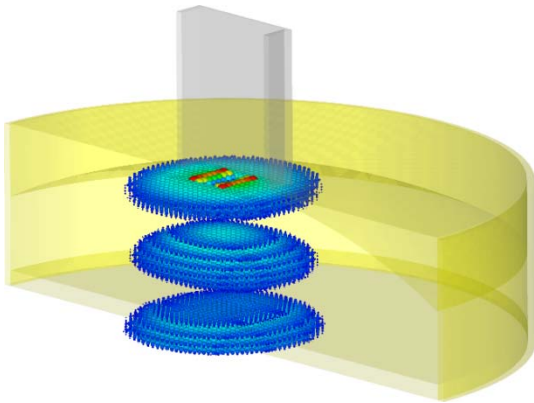


**Figure S 14:** 3D magnetic field distribution of the fourth mode occurring at 35 GHz in our FPR.

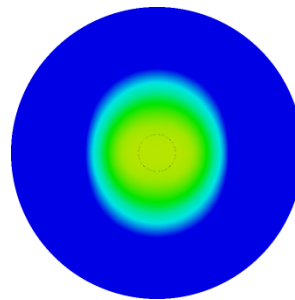


**Figure S 15:** 2D magnetic field distribution at the bottom mirror of the fourth mode occurring at 35 GHz in our FPR simulated .

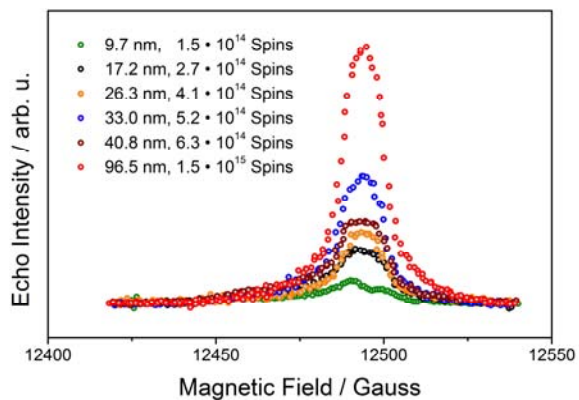


**Figure S 16** Echo detected EPR spectra recorded at 35 GHz and 7K of thin films of 5% BDPA in PMMA spin coated on a silicon substrate.

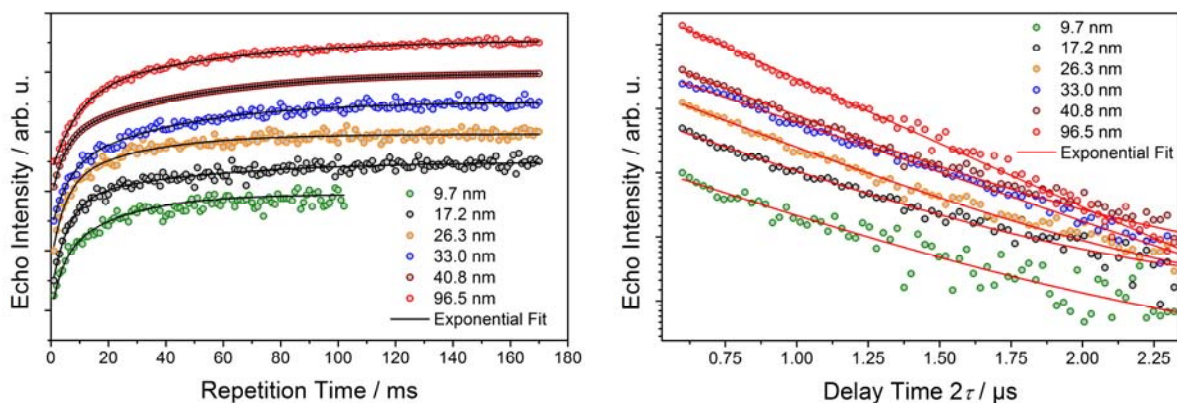


**Figure S 17.** Saturation recovery (left) and Hahn echo (right) decay curves recorded at 35 GHz and 7K of thin films of 5% BDPA in PMMA spin coated on a silicon substrate together with monoexponential fits.

**Table S 2.** Spin-lattice relaxation ( $T_1$ ) and phase memory ( $T_m$ ) times derived from fits of the monoexponential decay curves shown in Figure S17

Film thickness / nm	$T_1$ / ms	$T_m$ / $\mu$ s
9.7	$23 \pm 5$	$0.65 \pm 0.04$
17.2	$37 \pm 8$	$0.58 \pm 0.02$
26.3	$29 \pm 3$	$0.55 \pm 0.01$
33.0	$40 \pm 2$	$0.640 \pm 0.005$
40.8	$46 \pm 2$	$0.55 \pm 0.01$
96.5	$53 \pm 3$	$0.492 \pm 0.006$

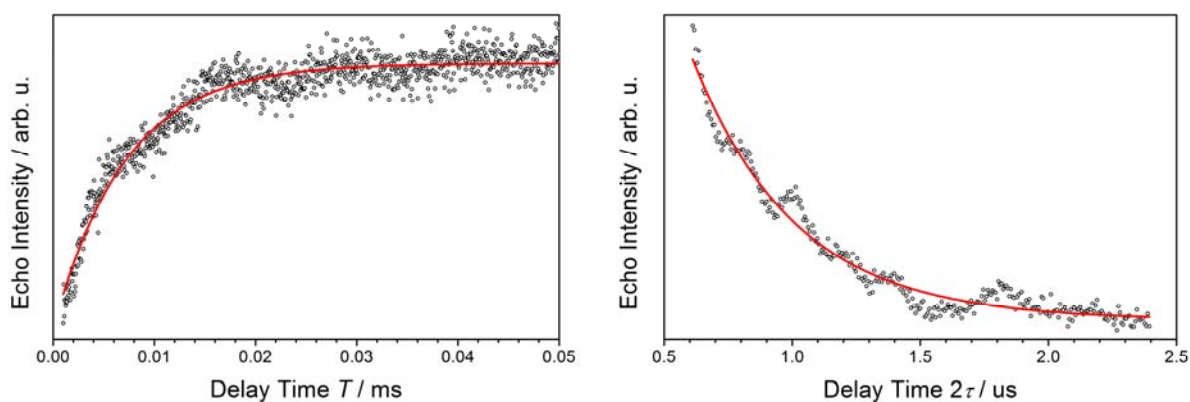


**Figure S 18.** Inversion recovery (left) and Hahn echo (right) decay curves recorded at 35 GHz and 7K of a 60 nm thick film of CuPc:H<sub>2</sub>Pc (ca. 1:5) on sapphire at 7K on substrate together with monoexponential fits.

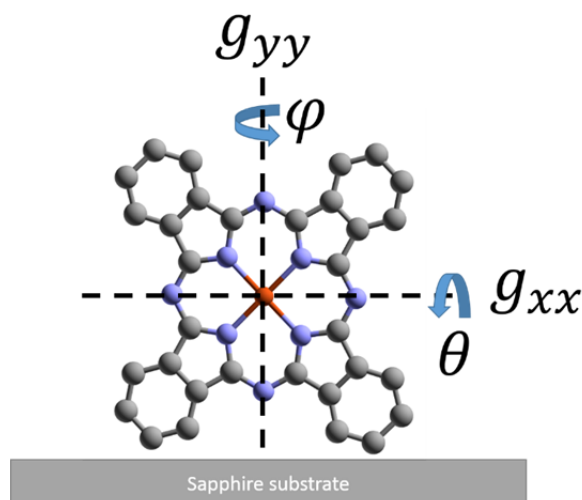
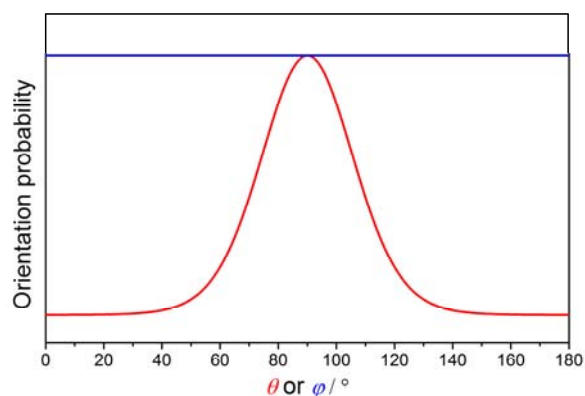
### Simulation of the pulsed EPR spectrum of the 60 nm film of CuPc:H<sub>2</sub>Pc at 7 K and 35 GHz

The pulsed EPR spectrum was simulated with the Matlab package *Easyspin* 5.2.25 using the spin Hamiltonian (eq. 1) with the parameters shown in Table S 3. CuPc molecules tend to ‘stand’ on technical substrates such as ITO and sapphire (see Figure S 19).<sup>1</sup> This induces a partial ordering of the molecules in the film, which can be taken into account in the powder averaging procedure in *Easyspin*. This was achieved by using the weighting function  $p(\theta) = e^{0.5\lambda(3\cos(\theta)^2-1)}$  for the angle  $\theta$ , which corresponds to the angle between the substrate surface normal with the  $g_{zz}$  axis. An ordering parameter  $\lambda = -4.5$  was used for the simulation, which results in the weighting function shown in Figure S 20. The surface interaction induces a slight rhombicity resulting in a  $g_{yy}$  value which is a little bit larger compared to the value observed in a powder of CuPc in H<sub>2</sub>Pc.<sup>2</sup>

$$\mathcal{H} = \mu_B \vec{B}^T \mathbf{0} \vec{g} \vec{S} + \vec{S}^T \mathbf{A}_{Cu} \vec{I} \quad (1)$$

**Table S 3** Spin Hamiltonian parameters used for the simulation of the pulsed EPR spectrum of the CuPc film

Sample	$g_{xx}$	$g_{yy}$	$g_{zz}$	$A_{Cu,xx}$	$A_{Cu,yy}$	$A_{Cu,zz}$	Ref
60 nm CuPc:H2Pc film (1:5)	2.039(1)	2.070(1)	2.158(1)	80(20)	80(20)	650(20)	This work
CuPc:H2Pc powder	2.0390(5)	2.0390(5)	2.1577(5)	-83(3)	-83(3)	-648(3)	<sup>2</sup>

**Figure S 19** Definition of the angles  $\varphi$  and  $\theta$  with respect to the molecular frame used for the simulation of the CuPc EPR spectrum.  $g_{zz}$  points in the direction of the viewer. In our experimental setup, the  $B_0$  field lies always in the plane of the substrate.**Figure S 20** Orientation probability used for the simulation of the CuPC EPR spectrum with respect to  $\theta$  and an arbitrary angle  $\varphi$  (red curve) and to  $\varphi$  with a fixed angle of  $\theta = 90^\circ$ 

Matlab code for the simulation of the partially ordered CuPc using *Easyspin 5.2.25*

```
clear

Sys.S=1/2;
Sys.g=[2.039,2.158,2.070]; %gzz has to be swapped with gyy in order
...to account for a preferred orientation within the xz plane using Exp.Ordering
Sys.Nucs='Cu';
Sys.A=[-83,-648,-83]; %Azz has to be swapped with Ayy, see above
Sys.lwpp=8;

Exp.Range=[1100 1260];
Exp.mwFreq=35;
Exp.Harmonic=0;
Exp.Ordering=-4.5 %Preferential ordering in the xz-Plane

pepper(Sys,Exp);
```

## AFM measurements

The thickness of the PMMA films with 5% BDPA was determined by scratching the surface with a wooden needle and measuring the height profile at the edge of the scratch using AFM. Figure S 21 shows a microscope picture of such a scratch and Figure S 22 the corresponding AFM measurement. Figure S 23 - Figure S 28 show the resulting height profiles of all the films which are discussed in the main part of the article.

The thickness of the CuPc:H<sub>2</sub>Pc film was determined at an edge where the substrate was not covered due to masking of the substrate by the sample holder in the evaporation chamber. Fig shows the sapphire substrate with the film, fig shows the AFM measurement and fig shows the resulting profile along which the thickness was determined.

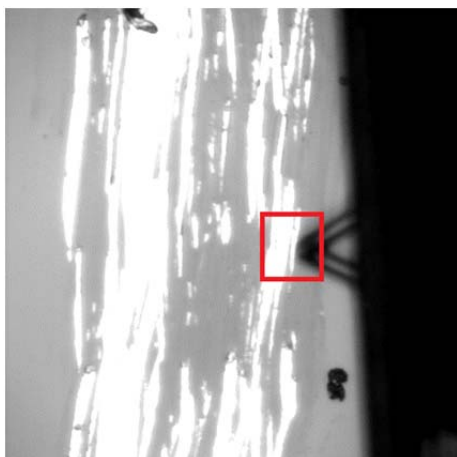


**Figure S 21** Microscope picture of a PMMA film scratched by a wooden needle. The area of the AFM measurement is highlighted by a red square, the AFM tip is visible as well (black triangle, out of focus).

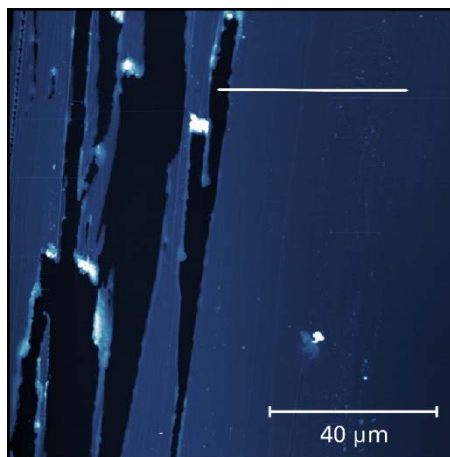


**Figure S 22** AFM measurement of the film shown in Figure S 21. The white line in the upper right part of the image shows an exemplary track along which the thickness was determined (Figure S 23 - Figure S 28)

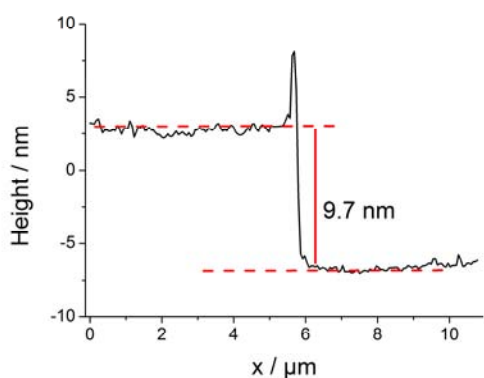


**Figure S 23** Height profile of a film spin coated on silicon from a solution of 2 G/L PMMA in toluene containing 5 w. % BDPA (wrt PMMA). Measurements were performed in the vicinity of a scratch induced by a wooden needle. The film thickness was determined at the edge of the scratch.

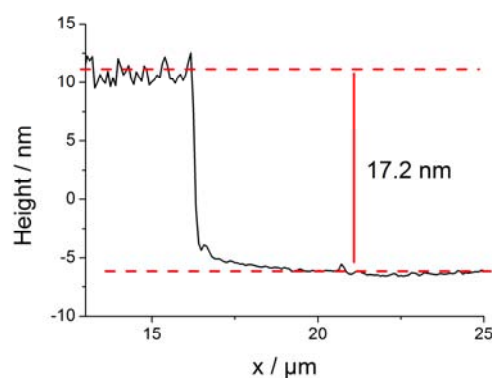


**Figure S 24** Height profile of a film spin coated on silicon from a solution of 4 G/L PMMA in toluene containing 5 w. % BDPA (wrt PMMA). Measurements were performed in the vicinity of a scratch induced by a wooden needle. The film thickness was determined at the edge of the scratch.

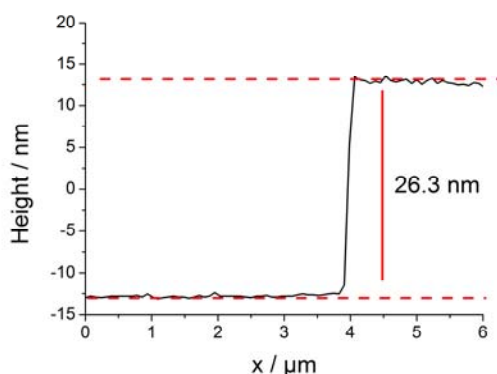


**Figure S 25** Height profile of a film spin coated on silicon from a solution of 6 G/L PMMA in toluene containing 5 w. % BDPA (wrt PMMA). Measurements were performed in the vicinity of a scratch induced by a wooden needle. The film thickness was determined at the edge of the scratch.

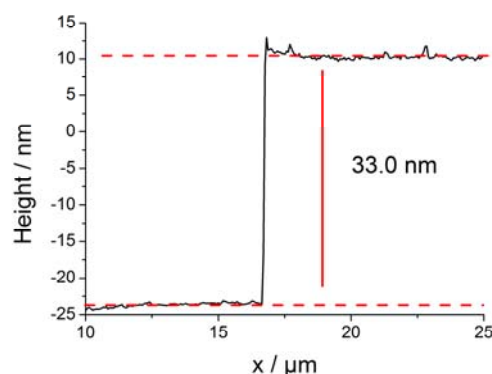


**Figure S 26** Height profile of a film spin coated on silicon from a solution of 8 G/L PMMA in toluene containing 5 w. % BDPA (wrt PMMA). Measurements were performed in the vicinity of a scratch induced by a wooden needle. The film thickness was determined at the edge of the scratch.

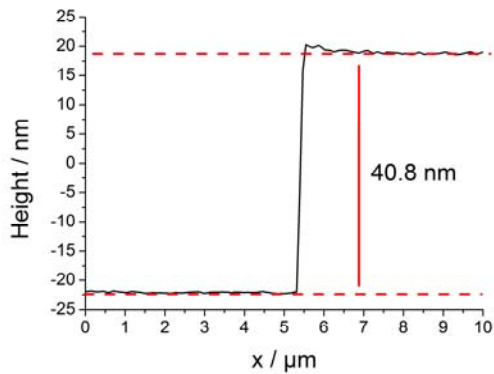


**Figure S 27** Height profile of a film spin coated on silicon from a solution of 10 G/L PMMA in toluene containing 5 w. % BDPA (wrt PMMA). Measurements were performed in the vicinity of a scratch induced by a wooden needle. The film thickness was determined at the edge of the scratch.

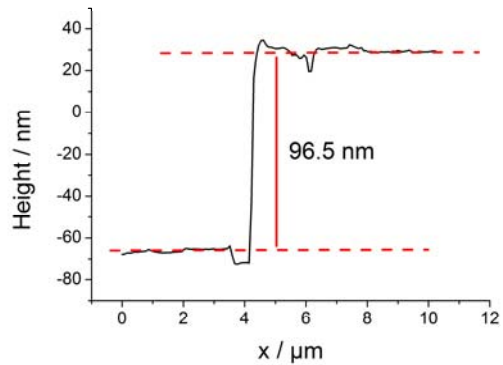


**Figure S 28** Height profile of a film spin coated on silicon from a solution of 20 G/L PMMA in toluene containing 5 w. % BDPA (wrt PMMA). Measurements were performed in the vicinity of a scratch induced by a wooden needle. The film thickness was determined at the edge of the scratch.

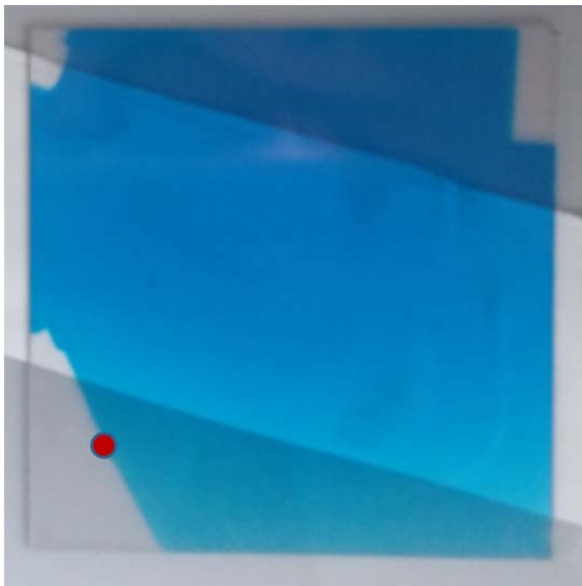


**Figure S 29** Image of the CuPc:H<sub>2</sub>Pc film on sapphire. AFM measurements were performed at the edge marked by the red dot.

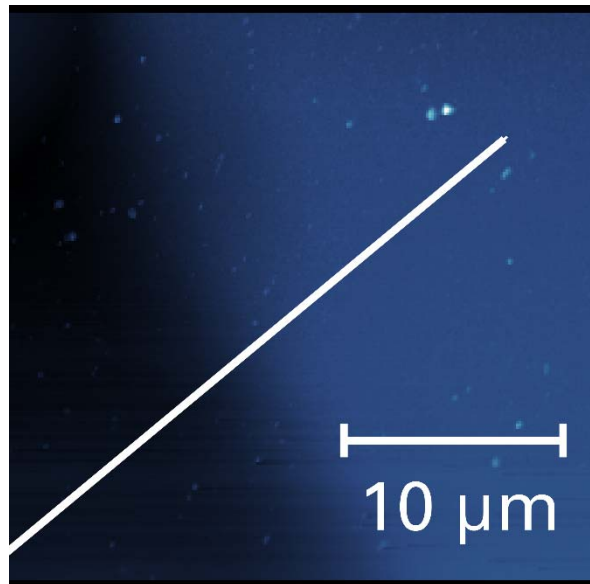


**Figure S 30** AFM measurement of the CuPc:H<sub>2</sub>Pc film shown in Figure S 29 at the edge marked by the red dot. Figure S 31 shows the profile along the included white solid line.

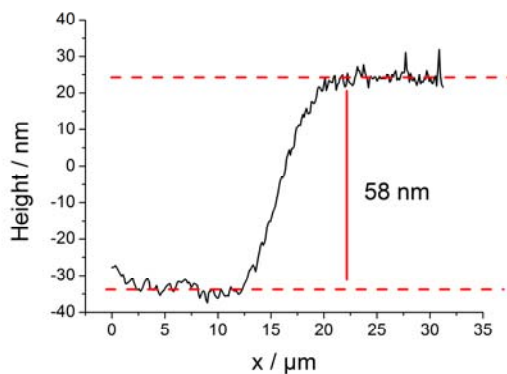


**Figure S 31** Height profile of the CuPc:H<sub>2</sub>Pc film along the white line in Figure S 30. The film thickness is about 60 nm.

## References

1. H. Peisert, T. Schwieger, J. M. Auerhammer, M. Knupfer, M. S. Golden, J. Fink, P. R. Bressler and M. Mast, *J. Appl. Phys.*, 2001, **90**, 466-469.
2. C. Finazzo, C. Calle, S. Stoll, S. Van Doorslaer and A. Schweiger, *Phys. Chem. Chem. Phys.*, 2006, **8**, 1942-1953.